Mechanism-Based Inactivation of Thioredoxin Reductase from *Plasmodium falciparum* by Mannich Bases. Implication for Cytotoxicity†

Elisabeth Davioud-Charvet,‡,§,|| Michael J. McLeish,‡ Donna M. Veine,§ David Giegel,⊥,# L. David Arscott,§ Adriano D. Andricopulo,‡,△ Katja Becker,▽ Sylke Müller,○ R. Heiner Schirmer,◇ Charles H. Williams, Jr.,*,§ and George L. Kenyon*,‡

College of Pharmacy, University of Michigan, 428 Church Street, Ann Arbor, Michigan 48109-1065, Department of Biological Chemistry, Medical School, University of Michigan, 3301B MSRB III, Ann Arbor, Michigan 48109-0606, Discovery Technologies, Pfizer Global Research and Development, Ann Arbor, Michigan 48105, Interdisciplinary Research Center, Giessen University, Heinrich Buff-Ring 26-32, D-35392 Giessen, Germany, Wellcome Trust Biocentre, University of Dundee, Dundee DD1 5EH, U.K., and Biochemie-Zentrum der Universität Heidelberg, Im Neuenheimer Feld 504, D-69120 Heidelberg, Germany

Received July 31, 2003; Revised Manuscript Received September 16, 2003

ABSTRACT: Thioredoxin reductase (TrxR) is the homodimeric flavoenzyme that catalyzes reduction of thioredoxin disulfide (Trx). For *Plasmodium falciparum*, a causative agent of tropical malaria, TrxR is an essential protein which has been validated as a drug target. The high-throughput screening of 350000 compounds has identified Mannich bases as a new class of TrxR mechanism-based inhibitors. During catalysis, TrxR conducts reducing equivalents from the NADPH-reduced flavin to Trx via the two redox-active cysteine pairs, Cys88-Cys93 and Cys535′-Cys540′, referred to as N-terminal and C-terminal cysteine pairs. The structures of unsaturated Mannich bases suggested that they could act as bisalkylating agents leading to a macrocycle that involves both C-terminal cysteines of TrxR. To confirm this hypothesis, different Mannich bases possessing one or two electrophilic centers were synthesized and first studied in detail using glutathione as a model thiol. Michael addition of glutathione to the double bond of an unsaturated Mannich base (**3a**) occurs readily at physiological pH. Elimination of the amino group, promoted by base-catalyzed enolization of the ketone, is followed by addition of a second nucleophile. The intermediate formed in this reaction is an α,β-unsaturated ketone that can react rapidly with a second thiol. When studying TrxR as a target of Mannich bases, we took advantage of the fact that the charge-transfer complex formed between the thiolate of Cys88 and the flavin in the reduced enzyme can be observed spectroscopically. The data show that it is the C-terminal Cys 535′-Cys540′ pair rather than the N-terminal Cys88-Cys93 pair that is modified by the inhibitor. Although alkylated TrxR is unable to turn over its natural substrate Trx, it can reduce low M_r electron acceptors such as methyl methanethiolsulfonate by using its unmodified N-terminal thiols. On the basis of results with chemically distinct Mannich bases, a detailed mechanism for the inactivation of TrxR is proposed.

Thioredoxin reductase (TrxR)[1] catalyzes the reduction of oxidized thioredoxin (Trx) by NADPH, according to the equation:

$$\mathrm{NADPH} + \mathrm{Trx(S)_2} \rightleftarrows \mathrm{NADP^+} + \mathrm{Trx(SH)_2} \qquad (1)$$

Trx is a M_r 12000 protein containing a redox-active pair of cysteine residues. Its wide distribution in nature attests to its physiological importance as a disulfide reductant which is crucial in processes such as ribonucleotide reduction and transcription factor modulation (*1*). TrxR is a member of the disulfide reductase enzyme family that includes glutathione reductase (GR), lipoamide dehydrogenase, and NADH peroxiredoxin reductase. There are two forms of

† This work was supported by the Office of the Vice President for Research, University of Michigan (M.J.M.), by the Centre National de la Recherche Scientifique (E.D.-C.), by Grants 39552 (G.L.K.) and 21444 (C.H.W.) from the National Institute of General Medical Sciences, by the Health Services and Research Administration of the Department of Veterans Affairs (C.H.W.), and by Grants BE1540/7-4 (K.B.) and BE2554/1-1 and SCHI102/8-1 (R.H.S.) from the Deutsche Forschungsgemeinschaft. S.M. is a Wellcome Senior Fellow.

* To whom correspondence should be addressed. C.H.W.: phone, (734) 647-6989 (voice mail); fax, (734) 763-4581; e-mail, chaswill@umich.edu. G.L.K.: phone, (734) 764-7312; fax, (734) 763-2022; e-mail, gkenyon@umich.edu.

‡ College of Pharmacy, University of Michigan.

§ Department of Biological Chemistry, Medical School, University of Michigan.

|| Present address: Biochemie-Zentrum der Universität Heidelberg, Im Neuenheimer Feld 504, D-69120 Heidelberg, Germany.

⊥ Discovery Technologies, Pfizer Global Research and Development.

Present address: MitoKor, 11494 Sorrento Valley Road, San Diego, CA 92121.

△ Present address: Center for Structural Molecular Biotechnology, Universidade de São Paulo, São Paulo, Brazil.

▽ Interdisciplinary Research Center, Giessen University.

○ Wellcome Trust Biocentre, University of Dundee.

◇ Biochemie-Zentrum der Universität Heidelberg.

[1] Abbreviations: CTC, charge-transfer complex; 3-DAP, 3-(dimethylamino)propiophenone; DMSO, dimethyl sulfoxide; DTNB, 5,5′-dithiobis(2-nitrobenzoic acid); DTT, dithiothreitol; ESI-MS, electrospray ionization mass spectrometry; E_{ox}, enzyme with the flavin and redox-active disulfide in the oxidized state; EH_2, two-electron-reduced enzyme; EH_4, four-electron-reduced enzyme; GR, glutathione reductase; GSH, reduced glutathione; MMTS, methyl methanethiolsulfonate; Trx, oxidized thioredoxin (thioredoxin disulfide); TrxR, thioredoxin reductase.

10.1021/bi0353629 CCC: $25.00
Published on Web 10/21/2003

TrxR in nature, the so-called low and high M_r forms. In addition to M_r the two forms differ in another important respect: the mode for transfer of reducing equivalents from the apolar milieu of the flavin to the more polar surroundings needed for dithiol−disulfide interchange (*2*).

Plasmodium falciparum is a causative agent of malaria. TrxR from *P. falciparum* has been cloned and expressed in *Escherichia coli* (*3*, *4*) and characterized as a high M_r form (*5*) similar to the human orthologous enzyme. TrxR is involved in maintaining an adequate reducing environment and defense against oxidative stress in *P. falciparum*. The unusual sensitivity of this organism to reactive oxygen species makes TrxR a promising drug target; it was recently shown that TrxR is essential for the survival of the parasites, validating the protein as a suitable target for drug design (*6*, *7*). The enzyme is not only of interest in parasitic organisms but is also considered as a potential drug target in the search for new anticancer chemotherapy (*8*). Indeed, TrxR is elevated about 10-fold in tumor cells compared with normal cells, and this is due not only to the need for higher amounts of deoxyribonucleotides but also for detoxification of reactive oxygen species (*2*, *9*).

It has been shown that the residues Cys88 and Cys93 represent the N-terminal redox-active site of *P. falciparum* TrxR (*5*). The sequence around this active cysteine pair is highly conserved in high M_r TrxR, including human TrxR. In contrast, the protein sequences differ profoundly at the C-terminal redox center where human TrxR contains a cysteine-selenocysteine pair (Cys495′-Sec496′) (*9*) while the parasitic TrxR has two cysteine residues (Cys535′ and Cys540′) separated by four amino acids (*3*, *4*). Reductive titrations of mutants derived by site-directed mutagenesis indicate that the C-terminal redox-active residues Cys535′-Cys540′ are in redox communication with the active Cys88-Cys93 pair of the other subunit (*10*−*12*). The clear chemical difference between the Cys-SeCys in human TrxR and the Cys-x−x-x−x-Cys in *P. falciparum* TrxR should be the basis for the design of inhibitors that specifically interact with the parasite enzyme.

In catalysis by TrxR, reducing equivalents are transferred from NADPH to the *re* face of the flavin and from the *si* face of the flavin to the N-terminal disulfide and thence to the C-terminal disulfide (*P. falciparum* TrxR) or selenosulfide (human TrxR) of the other subunit; finally, Trx is reduced by the C-terminal dithiol (Scheme 1). The function of each N-terminal thiol can be assigned by analogy to other members of the enzyme family: Cys88 initiates dithiol−disulfide interchange and Cys93 interacts closely with the flavin (*13*, *14*). High M_r TrxR can accept a total of three reducing equivalents of two electrons per active site, one for the flavin and one for each disulfide. NADPH only reduces the enzyme to the four-electron-reduced state. The spectra of two-electron- and four-electron-reduced forms, EH_2 and EH_4, are characterized by a charge-transfer complex (CTC) observed as a shoulder around 540 nm; the flavin-interacting thiol of Cys93 is the donor, and flavin is the acceptor (*15*). EH_2 and EH_4 are the predominant forms of TrxR in vivo when the enzyme is turning over substrate or at rest. Thus, these enzyme species are of special interest as targets of TrxR inhibitors (*16*).

The Mannich reaction is one of the most important C−C bond-forming reactions in organic chemistry and is widely used for the preparation of β-amino ketones and aldehydes. Mannich bases are versatile synthetic intermediates used in various transformations to prepare Michael acceptors via elimination of the amine moiety (*17*). Although different Mannich bases are used as drugs or drug candidates in medicine, very few studies have addressed the identification of the molecular targets and their mechanism of action. Dimmock and colleagues have published an important rationale (*18*) for understanding structure−cytotoxicity relationships and the mode of action of unsaturated Mannich bases at the chemical and cellular levels, but specific targets have not yet been identified. As shown in Scheme 2a, there is an initial attack by a thiol at the olefinic bond (intermediate A) followed by deamination of the monothiol adduct (intermediate B) and addition of a second thiol to the generated double bond (product C). This cascade of events could be the source of a sequential cytotoxicity which might be more damaging to neoplastic cells than normal tissues.

In this paper, we describe the mechanism-based inactivation of *P. falciparum* TrxR by unsaturated Mannich bases and suggest a putative mechanism based on mass spectrometric analysis of (di)thiol−Mannich base adducts and the spectroscopic properties of the flavoenzyme undergoing inactivation. The rationale for the synthesis of the compounds used in this study was based on high-throughput screening of 350000 compounds from the Pfizer library. The prototype for unsaturated Mannich bases is the Mannich base **3a**.

Scheme 1: Mechanism of *P. falciparum* TrxR-Catalyzed Trx Reduction[a]

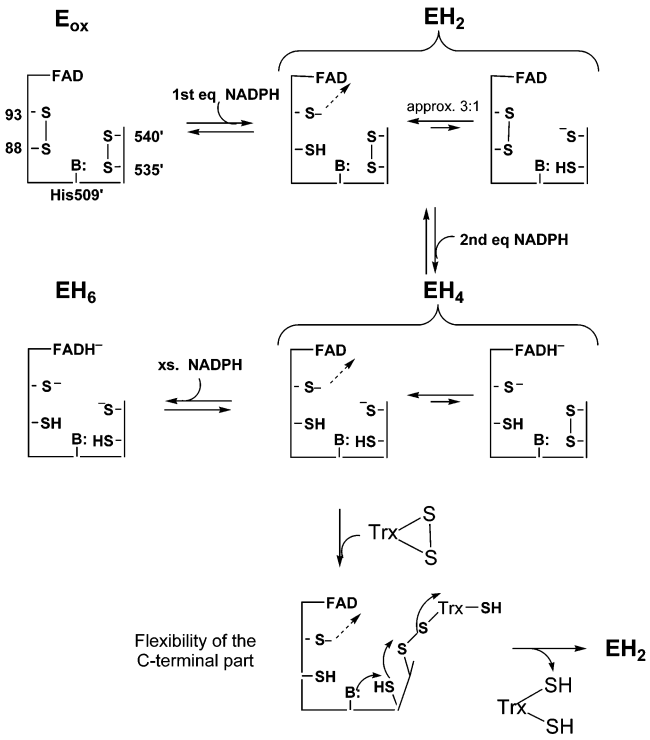

[a] The four groups comprising the active site are shown, FAD, the N-terminal redox-active disulfide (Cys88-Cys93), the C-terminal disulfide (Cys535′-Cys540′ from the other polypeptide chain), and the base catalyst, His509′ (also from the other polypeptide chain). The dashed arrow indicates charge transfer between the thiolate of Cys93 and FAD. $Trx(S)_2$ and $Trx(SH)_2$ are the oxidized and reduced forms of the substrate, respectively. The enzyme cycles in catalysis between the EH_4 and EH_2 forms (*37*).

Scheme 2: Postulated Reactivity of Unsaturated Mannich Bases versus Saturated Mannich Bases toward Nucleophilic Attack by Thiols[a]

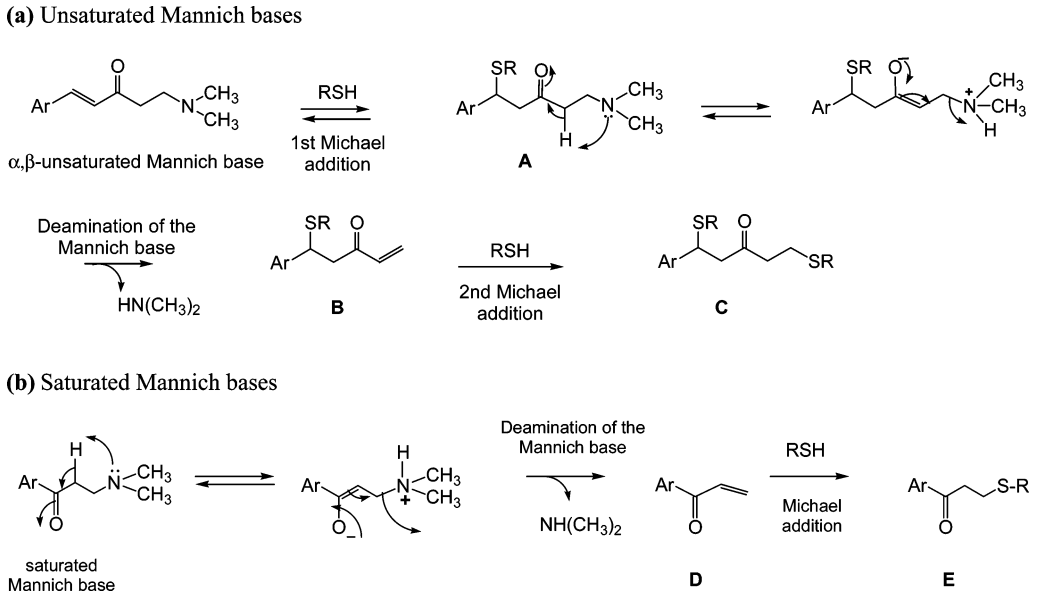

[a] Ar = aryl.

To evaluate the importance of two electrophilic sites of unsaturated Mannich bases for enzyme inactivation, an α,α-dimethyl-*β*-amino ketone **4** for which deamination is not possible and the saturated Mannich base 3-(dimethylamino)-propiophenone (3-DAP) were considered as key controls in the spectroscopic and kinetic studies. It was found that unsaturated Mannich bases inactivated TrxR in a rather specific manner when compared with saturated Mannich bases; the overall data enabled us to propose a mechanism for TrxR inactivation and to discuss their physiological relevance with respect to cytotoxicity.

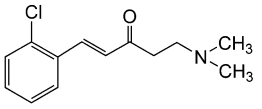
3a

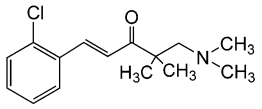
4

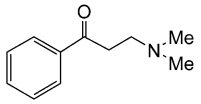
3-DAP

EXPERIMENTAL PROCEDURES

Reagents. NADPH was purchased from Sigma Chemical Co. (St. Louis, MO). 3-DAP hydrochloride (Aldrich D,-14480-0) and dithiothreitol (DTT) were purchased from Aldrich Chemical Co. (Milwaukee, WI). All other reagents and buffer salts were of the highest quality available and were purchased from Biomol, Boehringer, or Sigma. All experiments were conducted in 100 mM potassium phosphate buffer, pH 7.0, unless otherwise indicated.

Enzymes. Recombinant *P. falciparum* TrxR was purified as previously reported (*11*). One unit of TrxR activity is defined as the consumption of 1 μmol of NADPH/min ($\epsilon_{340\ nm}$ = 6.22 mM^{-1} cm^{-1}) under conditions of substrate saturation. TrxR activity was determined in the 5,5′-dithiobis-(2-nitrobenzoic acid) (DTNB) reduction assay as follows: the enzyme was added to a reaction mixture consisting of 100 mM potassium phosphate, 2 mM EDTA, pH 7.4, and 3 mM DTNB; after the addition of 200 μM NADPH, the increase in absorbance was monitored at 412 nm and 25 °C (*19*). Using the DTNB assay, one unit of TrxR is defined as the NADPH-dependent production of 2 μmol of 5-thio-2-nitrobenzoate (ϵ_{412nm} = 13.6 mM^{-1} cm^{-1}). Concentrations of TrxR in E_{ox} form were determined by measuring the content of FAD-containing subunits (ϵ_{460nm} = 11.3 mM^{-1} cm^{-1}) (*20*). The enzyme stock solutions used for the kinetic determinations were pure as judged from a silver-stained SDS−PAGE and had specific activity of 2.8 units/mg in the DTNB assay.

Screening Procedures. The initial 350000 compounds were screened via a 96-well format consisting of two plates in an *x* and *y* grid of 10 compounds per well at ca. 30 μM (assuming an average MW of 300). The initial screen was performed using MMTS (*21*) as a substrate at the following final concentrations: 50 mM potassium phosphate, pH 7.6, 1 mM EDTA, 100 μM NADPH, and 500 μM MMTS. Stock solutions of MMTS were dissolved in dimethyl sulfoxide (DMSO), allowing a final concentration of DMSO in the MMTS assay of 0.5%. The concentration of *P. falciparum* TrxR was established at 4−5 nM. The reaction was monitored at 340 nm at 25 °C for a period of 5 min. The secondary screen of 1992 compounds was performed using the same MMTS assay but with one compound in each well. The resulting 114 compounds were characterized over the range of compound concentrations from 0.16 to 25 μM with both 500 μM MMTS and 500 μM *E. coli* Trx substituted for MMTS.

pH-Dependent Formation of Glutathione−Mannich Base Adducts. A solution of the Mannich base **3a** (12.8 mg, 0.046 mmol) in 1 mL of H_2O was mixed with a solution of glutathione (GSH) (14.35 mg, 0.046 mmol, 1 equiv). The resulting solution was stirred at 37 °C for 14 h. The solvent was removed by lyophilization to give 27.8 mg of white powder containing the glutathione monoadduct of **3a**, 1-(2-chlorophenyl)-1-glutathionylsulfanyl-5-(*N*-dimethylamino)-

pentan-3-one, along with unreacted starting materials, according to HPLC and mass spectrometry analysis. A solution of **3a** (46.9 mg, 0.17 mmol, 1 equiv) and GSH (105.8 mg, 0.34 mmol, 2 equiv) in 5 mL of 10 mM phosphate buffer, pH 8.0, was heated at 80 °C for 30 min, cooled, and then lyophilized to give 199.2 mg of white powder containing the glutathione mono- and diadducts of **3a**, along with unreacted starting materials, according to HPLC and mass spectrometry analysis.

Liquid Chromatography. The glutathione conjugates of **3a** were separated on a C18 Supelcosil LC-318 column (4.6 × 254 mm, 5 μm, 300 Å). Analytical HPLC was performed on a HPXL Rainin instrument equipped with a UV detector set at 280 nm. Compounds (1−2 mg) were dissolved in 500 μL of eluent A, described below, and 10 μL was injected. The following solvent systems were used: eluent A, 0.1% trifluoroacetic acid (TFA) in H_2O; eluent B, 0.1% TFA and 99.9% CH_3CN. HPLC retention times were obtained, at flow rates of 0.7 mL/min, using the following conditions: 100% eluent A for 5 min and then a gradient run to 60% eluent B over the next 40 min. HPLC analyses were performed by the Protein and Carbohydrate Structure Facility of the University of Michigan.

Mass Spectrometry. Electrospray ionization mass spectrometry (ESI-MS) was carried out by analyzing the different fractions collected from HPLC and using a VG platform (Micromass, U.K.) single-quadrupole mass spectrometer. ESI-MS analysis was performed in positive ion mode by the Protein and Carbohydrate Structure Facility of the University of Michigan.

Anaerobic Spectroscopy, NADPH Titrations, and TrxR Activity Assays. All reductive titrations were performed under anaerobic conditions at 25 °C. Anaerobiosis was achieved by alternately degassing under vacuum and equilibration with ultrapure argon for eight cycles as described previously (*22*). Enzyme solutions were protected from light during anaerobiosis and reductive titrations. NADPH stock solutions were prepared in 40 mM Tris base solution (pH 9.0) and were made anaerobic by argon flushing for 10 min prior to use. The concentration of anaerobic NADPH solution was determined spectrophotometrically at 340 nm ($\epsilon_{340nm} = 6.22$ mM^{-1} cm^{-1}). Absorption spectra were recorded on a HP 8452A spectrophotometer. All spectra were corrected for slight turbidity by subtracting absorbance between 800 and 820 nm. Typical experiments proceeded in three phases: first, 20−30 μM TrxR (contained in a cuvette with two side arms similar to that described previously in ref *22*) was reduced anaerobically in 100 mM sodium phosphate buffer, pH 7.0, by 1.1 or 2.2 equiv of NADPH (contained in a 100 μL gastight Hamilton syringe) forming the FAD−thiolate CTC; next, 2−10 equiv of Mannich base per FAD-containing subunit (10−20 mM inhibitor solution in 100% DMSO contained in one side arm of the cuvette) was added, and the effect on the CTC was followed; finally, the protein modified by the Mannich bases was titrated with additional NADPH, and again the effect of enzyme modification on the FAD−thiolate CTC was examined. The enzyme was reoxidized by opening the cuvette to air and tested for residual activity. In each titration experiment, two controls were prepared according to the same titration conditions over the same period of time and assayed for residual Trx reduction at the end of the titration. The first control, i.e., "control TrxR−NADPH", consisted of TrxR incubated with the same amount of NADPH as in the titration. The second control, i.e., "control TrxR−inhibitor", consisted of TrxR incubated with inhibitor but in the absence of NADPH. This study was performed using recombinant enzyme with a specific activity of 18 units/mg and >95% pure on SDS−polyacrylamide gel electrophoresis (data not shown). The specific activities of wild-type TrxR and inhibitor-reacted enzyme from titration experiments were determined in the Trx reduction assay. It was carried out at 25 °C in a 1 mL cuvette containing 100 mM phosphate buffer, pH 7.0, in the presence of 100 μM NADPH, 0.01−0.10 μM TrxR (unreacted and inhibitor-reacted TrxR), and 50 μM Trx. The change in absorbance was measured at 340 nm.

Steady-State Kinetic Parameters Using the MMTS Reduction Assay. All kinetic studies were carried out at 25 °C in a 1 mL volume. The assay mixtures contained 100 mM phosphate buffer, pH 7.0, 200 μM NADPH, ∼6 nM unmodified or alkylated TrxR, and 0.5−40 mM MMTS (1.99% final DMSO concentration was kept constant). Initial rates were determined from NADPH oxidation measured at 340 nm.

Enzymic Assays Used in Inhibitor Studies. All assays were conducted at 25 °C in a total assay volume of 1 mL. In each measurement, residual activity in the presence of inhibitor was compared to the activity of a control without inhibitor. As control we used an enzyme preincubated with the same amount of DMSO, showing that inactivation was due to inhibitor and not to DMSO. Stability of TrxR was satisfactory up to 3.1% DMSO.

Evaluation of K_i and Inhibition Type. The enzyme was added to an assay mixture consisting of 50 mM potassium phosphate, 1 mM EDTA, pH 7.6, 230 μM NADPH, DTNB, and inhibitor. The reaction was initiated with the addition of the enzyme (13 milliunits in 5 μL aliquots, 38 nM TrxR subunit final concentration), and the increase in absorbance at 412 nm was monitored (*23*). Inhibition constants and the type of inhibition were determined in duplicate; **3a**, 0, 10, and 50 μM; DTNB, 150−400 μM; the DMSO concentration was kept constant at 2.5%. K_m and V_{max} values were determined by fitting data to the Michaelis−Menten equation using a nonlinear regression analysis (*24*). Inhibition of DTNB reduction by **3a** was measured as a function of DTNB concentration, and the data were fitted to the equation for competitive inhibition: $V_{max}/v_i = 1 + (K_m/[DTNB])(1 + [I]/K_i)$.

IC_{50} Determinations from Time-Dependent Inactivation. The loss of *P. falciparum* TrxR or human GR activities in preincubation with the inhibitor and NADPH for 5 min was determined by monitoring DTNB reduction (*25*). Enzyme (∼1.5 μM) was allowed to react for 5 min at 25 °C in a final volume of 56.5 μL of 100 mM potassium phosphate buffer, pH 7.6, with 208 μM NADPH and the inhibitor. Final inhibitor concentrations in the preincubation mixture were 0−20 μM for **3a**, 0−10 μM for **5**, 0−100 μM for **3b**, **3c**, **4**, and 3-DAP in 1.9% DMSO. Samples (50 μL) of each reaction mixture were added to the DTNB reduction assay for determination of the residual activity; the reaction mixture consisted of 100 mM potassium phosphate buffer, pH 7.6, 208 μM NADPH, and 3 mM DTNB (3.1% DMSO final). The change in absorbance was monitored at 412 nm. TrxR or GR activities were also measured using the physiological

Scheme 3: Synthesis of the Unsaturated Mannich Bases **3a**−**c**, **4**, and **5**[a]

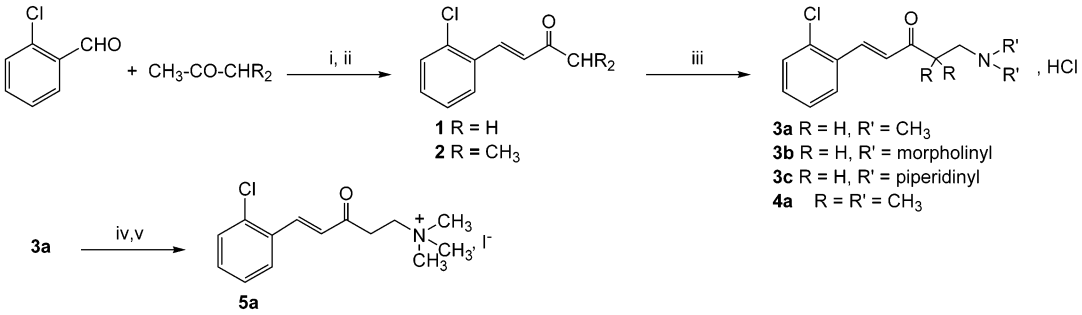

[a] Letters **a**−**c** reflect the alkyl substitution pattern: **a**, dimethylamine; **b**, morpholine; **c**, piperidine. Reagents: (i) 10% aqueous NaOH, room temperature; (ii) *p*-toluenesulfonic acid, toluene, reflux; (iii) paraformaldehyde, HNR_2·HCl, HCl, reflux; (iv) $NaHCO_3$; (v) CH_3I.

substrates Trx and GSSG, respectively, after preincubation with the inhibitor **3a** (0−10 μM, 1.9% final DMSO concentration) and NADPH for 5 min. The assay was started with 21 μM Trx or 121 μM GSSG. NADPH oxidation was monitored at 340 nm.

RESULTS

Screening. The high-throughput screen of 350000 compounds in the Pfizer library had identified 114 compounds that inhibit *P. falciparum* TrxR by at least 95% in an assay using NADPH as the donor substrate and MMTS as the acceptor (*21*). The 114 compounds were further tested again to allow calculation of IC_{50} values. A set of 34 compounds (not containing heavy metals) had IC_{50} values of <8.5 μM in the MMTS reduction assay. The structures for this set were made available according to our agreement with Pfizer. We tested the compounds in this set in an assay varying *E. coli* Trx as the acceptor substrate; only 15 inhibitors had IC_{50} values less than 18 μM. The discrepancies between the results with MMTS and those with *E. coli* Trx could be explained according to the observation that MMTS also interacts with the N-terminal cysteine pair and thus can be reduced even if the C-terminal Cys pair is blocked by an inhibitor (see Kinetic Parameters Using MMTS Reduction Assay). In the final stage, *P. falciparum* TrxR was compared to the human enzyme using *P. falciparum* Trx as the acceptor. Interestingly, *P. falciparum* Trx is a better substrate for the human enzyme than for *P. falciparum* TrxR (*19*). Six compounds showed IC_{50} values that were higher for the human enzyme than for the parasite enzyme; that is, they inhibited *P. falciparum* TrxR to a greater degree. It should be emphasized that, among the 15 most active inhibitors (IC_{50} values less than 18 μM), 13 compounds were Mannich bases, 9 saturated and 4 unsaturated (Scheme 2). Because the α,*β*-unsaturated ketones inhibited PfTrxR to a greater extent than the saturated ones, the structure of one of these (**3a**) was selected as a model to guide the synthesis of key analogues and to provide the rationale for TrxR inactivation. The commercial 3-DAP was also selected as a model for a saturated Mannich base.

Chemistry. The syntheses of **3a** and its analogues are given in Scheme 3. The starting 2-chlorobenzalacetones were prepared by Claisen−Schmidt condensation of 2-chlorobenzaldehyde and acetone, or 3-methyl-2-butanone, respectively. On the basis of Scheme 2, the rate of deamination should be inversely proportional to the basicity of the amine leaving group; a set of amines **a**−**c** (Scheme 3) displaying different pK_a values of the conjugated acids was employed in the Mannich reaction (*26*) to prepare **3a** and analogues from the appropriate *β*-arylvinyl alkyl ketone **1** or **2**, paraformaldehyde, and secondary amine hydrochloride. The electron density at the olefinic bond is reduced when the nitrogen atom is ionized with respect to the corresponding free bases; hence the quaternary ammonium salt **5** of the unsaturated Mannich base **3a** was expected to react with thiols more rapidly. It was prepared from the tertiary amine **3a** by reaction with methyl iodide according to the procedure of Edwards et al. (*27*).

pH-Dependent Formation of Glutathione−Mannich Base Adducts as Model Reactions. The α,*β*-unsaturated Mannich bases possess two electrophilic centers: the α,*β*-unsaturated ketone is obvious, but the other is masked and is revealed only after a base-dependent deamination of the *β*-amino ketone. Michael addition of a nucleophile to the double bond leads to the intermediate monoadduct (Scheme 2a, structure A). Elimination of the dimethylamino group, promoted by base-catalyzed enolization of the ketone, allows addition of a second nucleophile. The intermediate is another α,*β*-unsaturated ketone (Scheme 2a, structure B) which can react rapidly with a second thiol. Both elimination and addition reactions are pH-dependent, the optimum pH being linked to the pK_a values of the amine leaving group and of the nucleophilic species. The overall result is the addition of two nucleophiles (Scheme 2a, structure C). One equivalent of **3a** was reacted with 1 equiv of GSH for 14 h in H_2O at 37 °C (the resulting pH of the solution was found to be ∼4−5). The first Michael addition product shown in Scheme 2a (structure A) was confirmed by HPLC followed by ESI-MS and by NMR. The mass spectrum of the GSH conjugate of **3a** (see Supporting Information) showed an MH^+ at *m*/*z* 545.4, consistent with the addition of one molecule of GSH. Analysis of the ^{1}H NMR spectrum revealed the disappearance of both vinyl protons. No deamination−addition products (mono- or diadducts) were detected under these conditions of pH.

The known pH dependence of deamination and the fact that it is favored after addition of a first molecule of thiol indicated that the model reaction with GSH should be tested at higher pH; the most efficient conditions to observe the double adduct were 10 mM phosphate buffer, pH 8, at 80 °C for 30 min and 2 equiv of GSH. The resulting conjugates were analyzed by HPLC and ESI-MS, revealing two MH^+ peaks at *m*/*z* 545.2 (relative intensity 100), identified as the Michael adduct described above (structure A in Scheme 2a), and at *m*/*z* 807.2 (relative intensity 7.1%), identified as the

product of a double addition of GSH (structure C in Scheme 2a). This agrees with previous observations (*28*). The HPLC coupled to ESI-MS showed three major peaks with retention times of 19.01, 19.62, and 21.89 min, attributed to the starting Mannich base **3a** (30.1%), the monoadduct (37.5%), and the diadduct (8.5%), respectively. Under milder and more physiological conditions for glutathione conjugation of **3a** (37 °C, 18 h, 1 equiv of GSH), the presence of the diadduct was also observed and confirmed (data not shown).

Titration of NADPH-Reduced TrxR with α,β-Unsaturated Ketones and Mannich Bases: Rationale. In the mechanism depicted in Scheme 2a, the starting compound reacts rapidly but reversibly with thiols. While the reaction with α,β-unsaturated ketones (B) is known to be straightforward, complete, and irreversible, the reaction with unsaturated Mannich bases is 240-fold more rapid (*28*). The higher rate of addition is due to the presence of the strong electron-withdrawing ammonium group which lowers the electron density of the double bond. Retro-Michael addition to intermediate A is favored for the same reasons since the acidity of the protons α to the keto group is increased. In the case of the saturated Mannich bases (Scheme 2b), a different behavior is to be expected because an α,β-unsaturated ketone (structure D) is the only reactive intermediate; in the absence of a base provided by the enzyme, deamination is thought to occur by intramolecular abstraction of the α-hydrogen at a very slow rate.

The active site of the TrxR has all of the elements for this scenario: four cysteines as potential nucleophiles and a histidine as a catalyst for base-dependent deamination of unsaturated Mannich bases. On the basis of the different reactivities described above, it was expected that unsaturated Mannich bases would be much more specific for dithiols than for monothiols because the intramolecular reaction is favored. On the other hand, saturated Mannich bases would be attacked both by mono- and dithiols irreversibly.

To test these hypotheses, we compared the spectral properties of TrxR modified by different Mannich bases. The major aim was to determine the mechanism by which **3a** affected the activity of TrxR. The structure of a rat liver mutant TrxR shows that the C-terminal redox center is partially exposed to the solvent while the redox-active N-terminal thiol(s) is (are) more buried (*29*). Scheme 1 presenting the mechanism of Trx reduction catalyzed by TrxR is also fundamental to our hypothesis for the reaction of **3a** with TrxR. It is expected that the reagent will react with Cys540, the penultimate residue of TrxR, which is equivalent to the penultimate Sec in the mammalian enzyme.

*Reaction of the α,β-Unsaturated Mannich Base **3a** with the EH_2 Form of TrxR.* Figure 1 shows the spectrum of the oxidized enzyme (E_{ox}), the λ_{max} being 460 nm (curve 1). TrxR is converted to its predominant EH_2 form by 1 equiv of NADPH under anaerobic conditions (curve 2), as judged by the characteristic bleaching at 460 nm and the long-wavelength band centered around 540 nm where neither oxidized nor reduced flavin absorbs. The 540 nm band is due to reduction of the N-terminal disulfide bond between Cys93 and Cys88 and the formation of a thiolate−flavin CTC involving the thiol of Cys93 (Scheme 1). The two-electron-reduced TrxR was reacted with 2 equiv of **3a** (curve 3); the inset to Figure 1 shows the time-dependent loss of the CTC (at 540 nm) as the inhibitor reacted over a 106 min period.

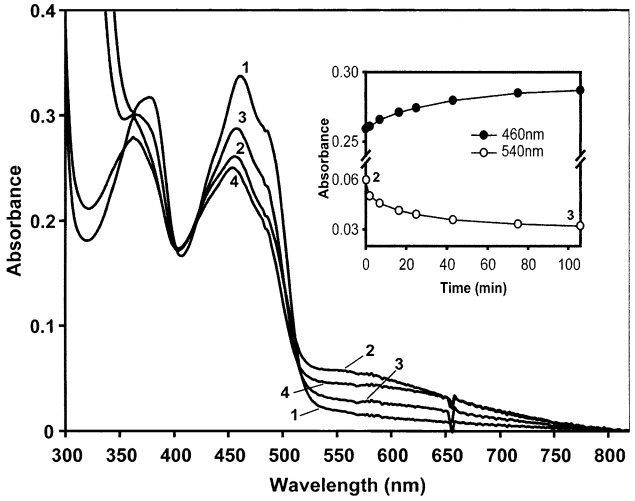

FIGURE 1: Reaction of **3a** and TrxR prereduced with 1 equiv of NADPH (EH_2). Oxidized TrxR (curve 1) was reduced with 1 equiv of NADPH per FAD to give EH_2 (curve 2). This prereduced EH_2 was reacted with 3 equiv of **3a**; the reaction product is represented by curve 3. The inset shows the time course of the reaction at 460 nm (●) and 540 nm (○) with **3a** (curve 3). A second equivalent of NADPH was added; the reaction product is represented by curve 4.

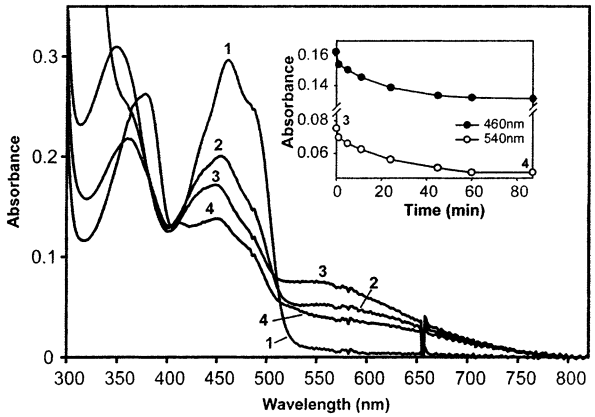

FIGURE 2: Reaction of **3a** and TrxR, prereduced with 2 equiv of NADPH (EH_4). Oxidized TrxR (curve 1) was reduced with 1 equiv of NADPH per FAD (curve 2) and then with a second equivalent of NADPH per FAD to give EH_4 (curve 3). Reaction of EH_4 with 3 equiv of **3a** yielded the product shown in curve 4. The inset shows the time course of the reaction (curve 3 to curve 4) at 460 nm (●) and 540 nm (○).

A subsequent addition of NADPH, however, led to reappearance of the CTC over a 25 min period (curve 4). The return of the CTC with further addition of NADPH indicated that reaction of **3a** did not occur with Cys93 but most likely with one of the C-terminal thiols (see also next section). The enzyme reoxidized with air had a normal spectrum and, importantly, was completely inactive with Trx as substrate; even incubation with 1 mM DTT for 29 min could not reactivate the modified enzyme.

*Reaction of the α,β-Unsaturated Mannich Base **3a** with the EH_4 Form of TrxR.* As shown in Figure 2, oxidized TrxR (curve 1) was converted to a four-electron-reduced form (EH_4), first with 1 equiv (curve 2) and then with 2 equiv of NADPH (curve 3), with concomitant formation of the full CTC. EH_4 was reacted with 3 equiv of **3a**. Comparison of curves 3 and 4 shows that CTC was lost as the inhibitor reacted but, importantly, only to the level expected for reduction of E_{ox} by 1 equiv of NADPH (see curve 2 as

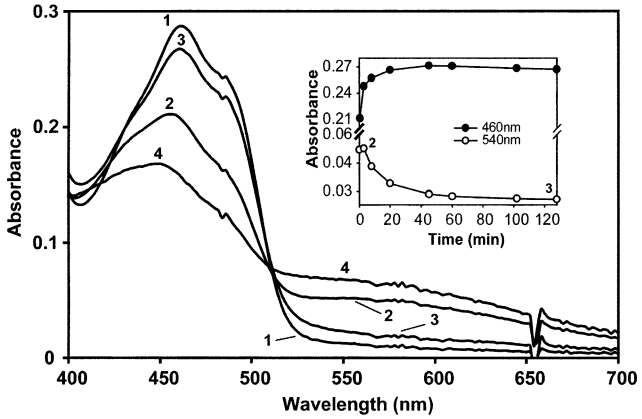

FIGURE 3: Reaction of **4** and TrxR prereduced with 1 equiv of NADPH (EH_2). Oxidized TrxR (curve 1) was reduced with 1 equiv of NADPH per FAD to give EH_2 (curve 2). This prereduced EH_2 was reacted with 3 equiv of **4**; the reaction product is represented by curve 3. The inset shows the time course of the reaction with **4** (curve 2 to curve 3) at 460 nm (●) and 540 nm (○). Addition of a second equivalent of NADPH restored the CTC (curve 4).

reference). The inset to Figure 2 shows this time-dependent loss of charge transfer at 540 nm. The reoxidized enzyme had a normal E_{ox} spectrum, was completely inactive in the Trx reduction assay, and could not be reactivated by excess DTT after 54 min.

*Reaction with α,α-Dialkyl Mannich Base **4** for Which Deamination Is Not Possible with the EH_2 Form of TrxR.* Compound **4** was synthesized for the purpose of studying TrxR inactivation with an analogue of **3a** where deamination is not possible. Three equivalents of **4** was reacted anaerobically with TrxR prereduced by 1 equiv of NADPH (Figure 3, curve 2 to curve 3). Superficially, the results are similar to those found with **3a**. A second equivalent of NADPH resulted in the full CTC with the expected higher absorbance at 540 nm (curve 4). The reoxidized enzyme exhibited a normal spectrum, but it was partially active (25% residual activity) in the Trx reduction assay, and full activity could be restored by treatment with 1 mM DTT for 23 min. As shown in the inset of Figure 3, reaction with **4** gave an initial increase in absorbance at 460 nm, suggesting that the rate of disappearance of the CTC did not follow the rate of apparent reoxidation of the flavin observable at 460 nm. An independent experiment confirmed the absence of significant spectral changes upon binding of **4** to E_{ox}. We will return to these observations in the Discussion.

Reaction of the Saturated Mannich Base 3-DAP with the EH_2 Form of TrxR. As shown in Figure 4, EH_2 (curve 2) was reacted with 3 equiv of 3-DAP (curve 3); the inset shows the time-dependent loss of the CTC (followed at 460 and 540 nm) as the inhibitor reacted; the expected concomitant increase in absorbance at 460 nm was not observed. Moreover, the kinetics observable at 540 nm did not follow those at 460 nm, as observed with **4**; however, whereas in the case of **4** there was a rapid increase at 460 nm followed by a further slow increase, with 3-DAP there was an immediate decrease at 460 nm followed by a further slow decrease. Addition of a further 1 equiv of NADPH restored the CTC absorbance (curve 4) and led to some flavin reduction. At the end of the experiment, the reoxidized enzyme had a normal E_{ox} spectrum and was found to be partially inactivated (36% residual activity) as shown in the

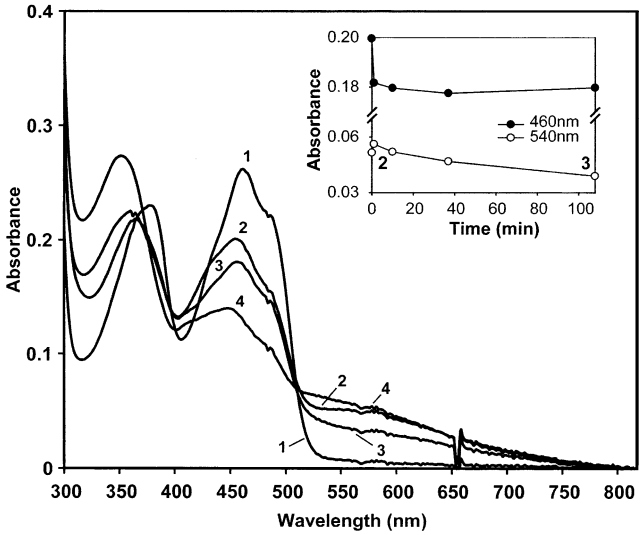

FIGURE 4: Reaction of 3-DAP and TrxR prereduced with 1 equiv of NADPH (EH_2). Oxidized TrxR (curve 1) was reduced with 1 equiv of NADPH per FAD to give EH_2 (curve 2). This prereduced EH_2 was reacted with 3 equiv of 3-DAP; the reaction product represented in curve 3 showed no reoxidation of the N-terminal thiols and a slow decrease of the CTC absorbance. The inset shows the time course of the reaction (curve 2 to curve 3) at 460 nm (●) and 540 nm (○). Addition of a second equivalent of NADPH restored the CTC (curve 4).

Table 1: Steady-State Kinetic Parameters of Unreacted *P. falciparum* TrxR, **3a**-Alkylated TrxR, and 3-DAP-Alkylated TrxR with MMTS as an Alternative Substrate[a]

enzyme	K_m (mM)	k_{cat} (s^{-1})	k_{cat}/K_m (M^{-1} s^{-1})
active wt TrxR[b]	2.77 ± 0.25	106 ± 3.1	38.4×10^3
3a-alkylated TrxR[c]	2.17 ± 0.16	45.5 ± 0.84	21.0×10^3
3-DAP-alkylated TrxR[d]	3.71 ± 0.42	51.3 ± 1.81	13.8×10^3

[a] All assays were carried out in duplicate at 25 °C in 100 mM phosphate buffer, pH 7.0, in the presence of 0.2 mM NADPH. [b] $K_m = 10.4 \pm 0.6$ μM, $k_{cat} = 51.7$ s^{-1}, and $k_{cat}/K_m = 5.0 \times 10^6$ M^{-1} s^{-1} in the assay based on *P. falciparum* Trx reduction (*19*). [c] Enzyme resulting from the NADPH titration experiment in the presence of 3 equiv of **3a** and found inactivated in the Trx reduction assay. [d] Enzyme resulting from the NADPH titration experiment in the presence of 10 equiv of 3-DAP and found inactivated in the Trx reduction assay.

Trx-based assay. The partially inhibited enzyme was completely inactivated by use of a further 7 equiv of reagent and could not be reactivated by exposure to 1 mM DTT for 82 min.

*Steady-State Kinetic Parameters of Unmodified TrxR, **3a**-Alkylated TrxR, and 3-DAP-Alkylated TrxR Using the MMTS Reduction Assay.* For these studies, we used MMTS as the acceptor substrate in the TrxR assay, replacing the natural substrate Trx. Interestingly, even the modified enzyme forms that showed no activity with Trx were partially active in the MMTS reduction assay, suggesting that the small, apolar MMTS could gain access to and react with Cys88 in the N-terminal part of the active site of unmodified enzyme or enzyme alkylated at the C-terminus. To test the hypothesis, we determined the kinetic parameters of unreacted TrxR, **3a**-alkylated TrxR, and 3-DAP-alkylated TrxR at increasing concentrations of MMTS (0.5−40 mM) and constant NADPH concentration. All three reactions followed Michaelis−Menten kinetics as summarized in Table 1. **3a**-alkylated TrxR and 3-DAP-alkylated TrxR showed decreased catalytic

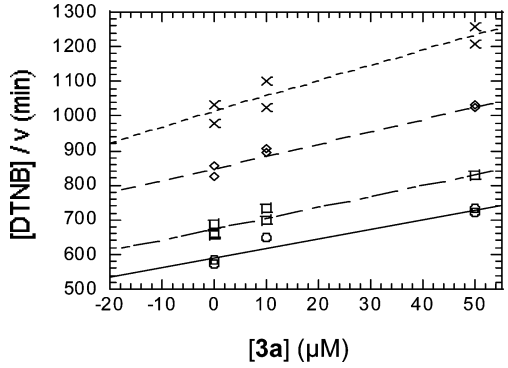

FIGURE 5: Cornish-Bowden diagram for the inhibition of TrxR by Mannich base **3a**. At DTNB concentrations in the range of 150−400 μM, the reversible competitive component of inhibition becomes evident. Upper to lower lines are for 400, 300, 200, and 150 μM DTNB. The K_m value for DTNB in the absence of inhibitor was 210.6 ± 10.4 μM. The K_i value for **3a** was determined as 147 ± 2.8 μM.

efficiency when compared to the untreated enzyme. The results confirmed (i) that MMTS is likely reduced in both the N-terminal and C-terminal parts of the active site at Cys88-Cys93 and Cys535′-Cys540′ of unmodified TrxR and (ii) that MMTS is reduced in the N-terminal active site of enzyme species alkylated at the C-terminal cysteine residues.

Inhibition Studies under Steady-State Conditions. The inhibition of TrxR by the unsaturated Mannich base **3a** showed an inactivation pattern characterized by a reversible component, i.e., competition with the substrate DTNB (Figure 5), as well as an irreversible component. The K_m and k_{cat}/K_m values for DTNB in the absence of inhibitor were 210 ± 10.4 μM and 2.8 × 10^6 M^{-1} min^{-1}, respectively. Apparent K_m values for DTNB were determined at different inhibitor concentrations of **3a**. A Cornish-Bowden diagram made the competitive component of the inhibition evident at DTNB concentrations ≤400 μM, as indicated by the parallel lines (Figure 5). By fitting the experimental data to the equation for competitive inhibition, the K_i value for the unsaturated Mannich base **3a** was determined to be 147 ± 2.8 μM.

To characterize the irreversible inhibition, 1.5 μM TrxR, reduced with 210 μM NADPH, was incubated with 0−10 μM **3a** for 0−60 min at 25 °C. Residual activity was assayed using the physiological substrate Trx at 21 μM. TrxR activity decreased markedly after preincubation with NADPH and **3a** in both a concentration- and time-dependent manner, indicating that the unsaturated Mannich base affected TrxR activity irreversibly. For a preincubation time of 5 min, the IC_{50} value was found to be 1.1 μM. This irreversible inhibition of TrxR is a fairly rapid process, as judged from the second-order rate constant evaluated as 2100 M^{-1} s^{-1} determined from the equation $d[E]/dt = k[E][I]$. It should be noted that reduction of the enzyme by NADPH is a prerequisite for irreversible inhibition. When TrxR was preincubated with the Mannich bases in the absence of NADPH, no inhibition was observed.

Using the same procedure with different Mannich bases (see structures in Scheme 3), TrxR activity was measured in the DTNB reduction assay. IC_{50} values were calculated from the concentration-dependent curves (Table 2). The presence of two electrophilic centers (unsaturated Mannich bases) appears to result in complete inactivation. A correlation was observed between the IC_{50} and the pK_a values of the amine leaving groups, with the exception of the morpholine derivative, where the bulky heterocycle and the presence of the oxygen atom could affect the binding to the active site.

Table 2: Inhibition of TrxR by Mannich Bases[a]

compd[a]	pK_a value of the amine leaving group	IC_{50} in DTNB reduction assay[b] (μM)
3a	10.77	1.9
3b	8.78	7.8
3c	11.24	15.5
5a	9.75	0.8
4a	10.77	reversible
3-DAP	10.77	15.4

[a] IC_{50} values for irreversible inhibition using the DTNB reduction assay; enzyme was incubated for 5 min at 25 °C with NADPH and varying inhibitor concentrations prior to the addition of DTNB. [b] The structures of compounds **3**−**5** are shown in Scheme 3.

To test the specificity for TrxR inhibition by the Mannich bases, we determined the inhibitory effects of the compounds on the mechanistically related human GR, which, unlike TrxR, has only an N-terminal redox-active cysteine pair, with only one of the two cysteine residues being partially exposed to the solvent. Inhibition was studied under the conditions used for TrxR. Human GR was only slightly inhibited by **3a** (10% at 970 μM **3a** versus 11% *P. falciparum* TrxR inhibition at 0.24 μM **3a**). As determined in the preincubation assay, **3a** inhibited human GR but with a second-order rate constant of 3.3 M^{-1} s^{-1}, that is, at least 650-fold lower than for TrxR. Thus, host GR and parasite TrxR are differentially inhibited.

DISCUSSION

Our findings provide evidence that unsaturated Mannich bases inactivate TrxR by interacting with the C-terminal redox-active cysteine residues of the protein (Scheme 4). The fact that the thiolate−flavin CTC decreases upon reaction with **3a** and returns when further NADPH is added indicates that the N-terminal thiols are not modified (see below). The results are supported by the finding that MMTS is still reduced by alkylated TrxR; although MMTS reacts preferentially with the C-terminal thiols, it can react with the N-terminal thiols as well (Table 1).

pH-Dependent Formation of Thiol−Mannich Base Adducts. Our data confirm the pH dependence of the formation of glutathione−Mannich base adducts. The first step, addition of the thiol to the β-arylvinyl ketone, leads to the formation of the monoadduct (Scheme 2a, structure A). This occurs at a far greater rate with the α,β-unsaturated Mannich bases than with corresponding α,β-unsaturated ketone analogues (structure B) (*28*). The second step involves deamination and addition reactions that are controlled by four parameters. On the basis of our studies the influence of each parameter can be rationalized as follows. First, deamination is pH-dependent because enolization is a prerequisite: the diadduct is generated at pH 8 but not at pH 4−5 in the model reaction with glutathione. Second, the basicity of the amine leaving group influences the rate of deamination since, as expected, inactivation increased with decreasing basicity of the amine leaving group, except for the morpholine derivative. This latter case illustrates the influence of the third parameter,

Scheme 4: Proposed Mechanism for TrxR Inactivation by the Unsaturated Mannich Base **3a**[a]

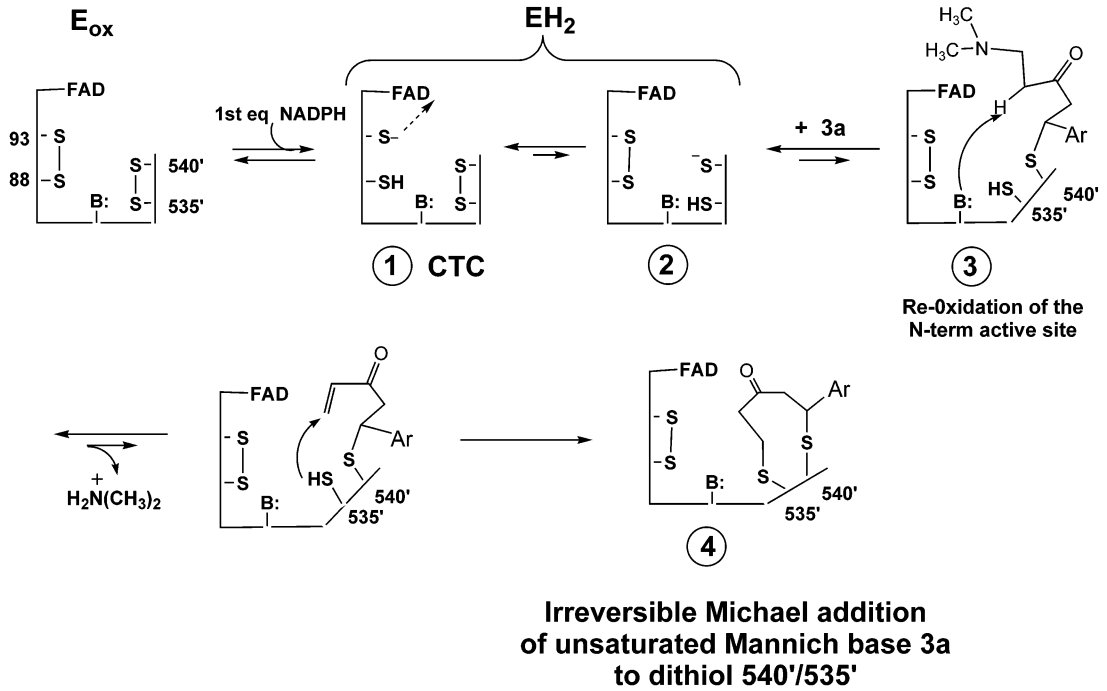

[a] Compound **3a** reacts with one of the EH_2 species reduced at the C-terminus, species **2**. Base-catalyzed deamination creates a second site for Michael addition, leading to the macrocyclic species **4**.

namely, the steric effects and/or the electrostatic repulsion. The steric restriction applies also to the interaction between the generated α,β-unsaturated ketone (intermediate B) and the nucleophile. That is, the fourth parameter is the influence of the basicity and nucleophilicity of the attacking thiol on the rate of S-alkylation which is expected to increase with low pK_a values. In other words, the concentration of thiolate in the inactivation process has to be considered with great care since the pK_a value of cysteine and selenocysteine residues can be as low as ca. 5 in the active site of an enzyme (*30*).

*Mechanism-Based Inactivation of TrxR by Unsaturated Mannich Bases **3a** and **4**.* Scheme 4 presents a putative mechanism for the inhibition of TrxR by the unsaturated Mannich base **3a**. The mechanism explains the observation that the enzyme is inhibited only when it is reduced to the EH_2 or EH_4 levels, which makes thiols available. It is known from the high extinction coefficient of the CTC that the equilibrium between the two EH_2 species, **1** and **2**, shown in Scheme 4 favors the CTC species **1**. We propose that the C-terminal thiols of TrxR are the reactive nucleophiles and that His509′ catalyzes the deamination of the reagent by promoting enolization of the keto group. The equilibrium between EH_2 species is shifted as **3a** reacts; as seen in Figure 1, the CTC decreases as **3a** reacts. The resulting inactivated enzyme is the macrocyclic species **4** most likely resulting from alkylation first at Cys540′ and then at Cys535′. Inhibition by **3a** cannot be reversed by DTT. The formation of macrocycles between unsaturated Mannich bases and dithiols is well documented in polymer chemistry (*31*). Also, a stable dithioarsine ring complex with vicinal dithiols has been previously described with 4-aminophenylarsine oxide (*32*, *33*).

Return of the CTC if more NADPH is added to species **4** in Scheme 4 supports our contention that the N-terminal thiols are not the site of reaction. Cys93 cannot have reacted since it is still able to act as the charge-transfer donor. We would argue that alkylation of Cys88 by as large an electrophile as **3a** would disrupt the CTC; this suggestion is supported by the behavior of the closely related enzyme lipoamide dehydrogenase. In this enzyme, the interchange thiol is at least 10-fold more reactive with electrophilic reagents than is the charge-transfer thiol. Reaction of the interchange thiol of lipoamide dehydrogenase with the relatively small reagent, iodoacetamide, leads to complete loss of the charge-transfer interaction (*13*). On the other hand, reaction of the analogous thiol of GR with iodoacetamide does not affect the charge transfer (*34*).

The mechanism for inhibition by **3a** requires that the carbon in the position α to the keto group has an acidic hydrogen in order for deamination to occur (Scheme 2a). In the case of the α,α-dimethyl-unsaturated Mannich base **4**, no deamination is possible. Scheme 5 shows our interpretation of the data in Figure 3. Compound **4** reacts with the EH_2 mixture as **3a** does for the first Michael addition, presumably at the most exposed thiol Cys540′ (species **3**). However, the subsequent reactions are different because there are no hydrogens to be abstracted from the carbon in the position α to the keto group of the β-amino ketone motif. Expulsion of the reagent by retro-Michael addition from the adduct can occur at a high rate, in accordance with reported glutathione dethiolation rates measured for the *N*-diethyl analogue of **4** (*35*, *36*). The propensity of the retro-Michael reaction accounts for the partial activity observed upon reoxidation of the reacted enzyme; the retro-Michael reaction also accounts for enzyme reactivation by excess DTT (Scheme 5). The lag at 540 nm and the increase in absorbance at 460 nm in the 3 min following addition of the reagent might result from minor alkylation at Cys88. The presence of free EH_2 in significant concentration is evidenced

Scheme 5: Proposed Mechanism for PfTrxR Inactivation by **4** and Reactivation by DTT[a]

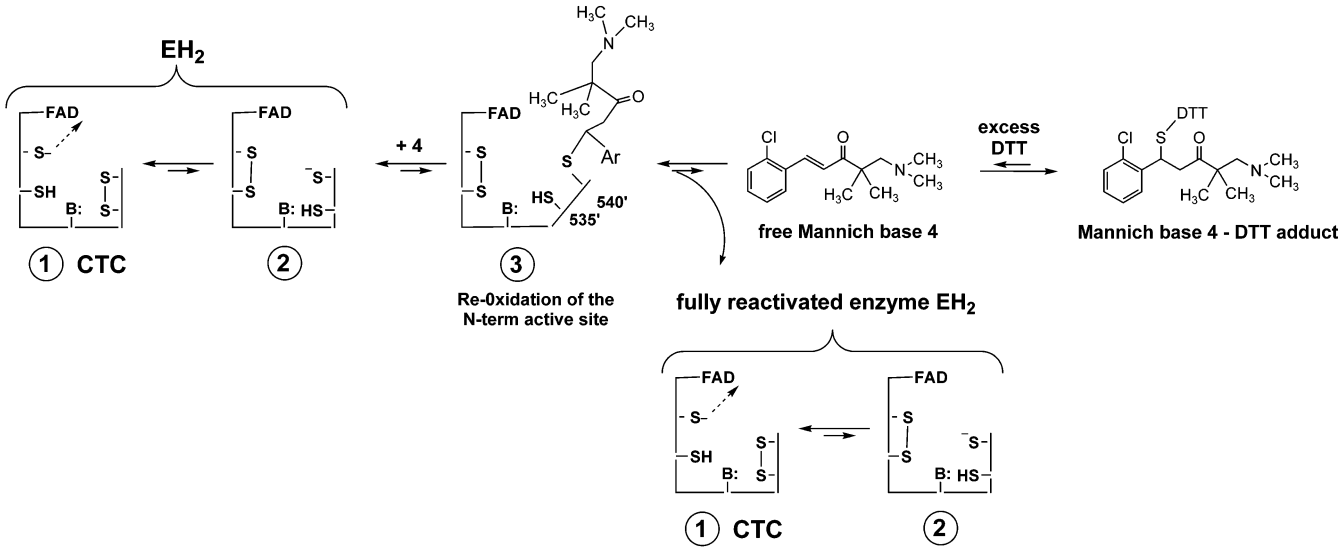

[a] Compound **4** reacts initially with prereduced enzyme just as **3a** does. Subsequent steps differ due to the absence of an acidic proton at the carbon α to the *β*-amino ketone motif and due to reversibility via a retro-Michael reaction. Ar = 2-chlorophenyl.

Scheme 6: Mechanism Proposed for PfTrxR Inactivation by Saturated Mannich Base 3-DAP[a]

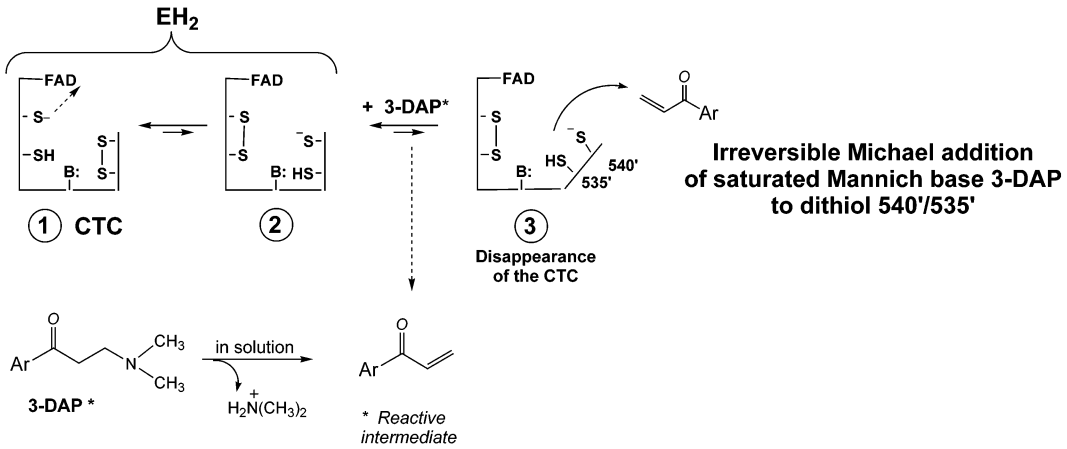

[a] The structure of the reactive intermediate generated in solution from 3-DAP is indicated by an asterick (see structure D in Scheme 2b).

by the formation of EH_4−CTC following addition of further NADPH. At the end of the reaction, addition of a large excess of DTT leads to complete reactivation of the enzyme by expulsion of the reagent via a retro-Michael reaction (Scheme 5). Reaction of the released reagent to form the DTT−**4** adduct shifts the equilibrium in favor of the retro-Michael reaction.

Mechanism-Based Inactivation of TrxR by Saturated Mannich Bases. The saturated Mannich base 3-DAP reacted more slowly with the enzyme than unsaturated Mannich bases. This accounts for the larger excess of reagent necessary to fully inactivate the enzyme, in agreement with the 8-fold higher IC_{50} value of 3-DAP (Table 2). Further treatment of the 3-DAP-reacted enzyme with 7 equiv of reagent was required for complete inactivation of TrxR. Comparison of the reactivity of the two classes of reagents, unsaturated (Scheme 2a) and saturated Mannich bases (Scheme 2b), will make the difference clear. First, saturated Mannich bases illustrated by 3-DAP undergo slow deamination in solution, leading to the formation of the reactive α,*β*-unsaturated ketone (Scheme 2b, intermediate D). We suggest that 3-DAP binds to the enzyme as do other Mannich bases and is deaminated following proton abstraction by His509′. The deamination is shown in Scheme 6 as occurring in solution. However, alkylation by 3-DAP is less efficient because the reactive intermediate is an α,*β*-unsaturated ketone with a lower reactivity toward thiols. Addition of the most exposed thiols to this reactive ketone might lead to multiple alkylation of TrxR, in agreement with the decrease of CTC absorbance at 540 nm (see inset, Figure 4). However, as observed with **4**, higher absorbance at 540 nm in the first 3 min after addition of the reagent (cf. insets, Figures 3 and 4) might be due to minor alkylation of Cys88. But in that case, no reversible interchange between Cys88 and C-terminal thiols is possible because addition of thiols to unsaturated ketones is irreversible (Scheme 2b). At the end of the experiment, the mixture of enzymic species accounts for the observed 36% residual activity in the Trx assay. Complete inactivation was reached after addition of a further 7 equiv of reagent (Scheme 6). The residual MMTS reduction activity of the resulting enzyme shows that the C-terminal cysteine pair is the major target of 3-DAP.

Implications for Cytotoxicity. Unsaturated Mannich bases can react spontaneously with thiols such as GSH that are

present in cells at high concentration, but the reaction is reversible. On the other hand, treatment of vicinal dithiols, as in the C-terminal redox center of TrxR, with unsaturated Mannich bases is much more favorable for entropic reasons; this reaction allows a more complete, specific modification of TrxR than is possible with the mono-thiol GSH, or glutathione reductase, where only one cysteine of the catalytic center is partially exposed while the other one is buried. An extensive series of Mannich bases possessing one or two sites for thiol alkylation was evaluated for cytotoxicity against various tumoral cell lines, showing that reagents capable of bisalkylation were more effective (*27*, *35*, *38*−*40*). This agrees with our results showing more efficient inactivation of TrxR by the unsaturated Mannich bases. Recent reports demonstrated that, in addition to having a cytotoxic effect, Mannich bases can induce apoptosis in several types of cells (*40*). GSH and reduced Trx levels are closely tied to apoptosis, especially in rapidly dividing cancer cells and parasites. We suggest that inactivation of human TrxR by unsaturated Mannich bases may be one of the causes of apoptotic death in human tumor cells (*41*−*48*). In contrast, saturated Mannich bases such as 3-DAP are much less specific; many low molecular weight thiols and enzymic thiol targets could indeed react irreversibly with these reagents.

Conclusions. Our results demonstrate for the first time the mechanism-based inactivation of reduced TrxR from *Plasmodium falciparum*, the predominant form of the enzyme in vivo, by Mannich bases. The putative mechanism for irreversible inactivation by α,β-unsaturated Mannich bases such as **3a** involves formation of an inactive macrocyclic species by bisalkylation, first of the C-terminal thiol of Cys540′ (the equivalent of SeCys in the human enzyme) and subsequently of Cys535′. Following the initial Michael addition, base-catalyzed enolization is probably promoted by His509′, allowing deamination and addition of the second thiol. The partial inhibition by the α,α-dialkyl Mannich base **4** for which deamination is not possible can be fully reversed by DTT. Reduction of the low M_r substrate MMTS is possible at the N-terminal interchange thiol Cys88 of C-terminally alkylated enzyme species. Saturated Mannich bases such as 3-DAP are less efficient and less specific inhibitors leading to multiple alkylation.

NOTE ADDED IN PROOF

A second base, His106, has been observed in the active site of TrxR of *Drosophila melanogaster*. Modeling His106 into the active site of the known three-dimensional structure of the rat liver enzyme juxtaposes it with respect to the C-terminal thiols just as His464 is juxtaposed toward the N-terminal thiols (*49*). This histidine residue is conserved in TrxR from *P. falciparum* as His137. It seems likely to us that His137 functions in the roles that we have ascribed to His509, for example, in the deprotonation of the **3a**−TrxR adduct prior to deamination.

ACKNOWLEDGMENT

We acknowledge the late Professor Vincent Massey, University of Michigan, for the use of his laboratory in the spectroscopic experiments and for many helpful suggestions. We thank Dr. Holger Bauer for initiating E.D.-C. to anaerobic titration experiments and Irene König, University of Heidelberg, as well as Elisabeth Fischer, University of Giessen, for excellent technical assistance.

SUPPORTING INFORMATION AVAILABLE

Details of chemical procedures (Scheme 1), analytical data of compounds **1**−**5**, and ESI-MS spectra of **3a**−glutathione conjugates. This material is available free of charge via the Internet at http://pubs.acs.org.

REFERENCES

1. Arnér, E. S., and Holmgren, A. (2000) *Eur. J. Biochem. 267*, 6102−6109.
2. Williams, C. H., Arscott, L. D., Müller, S., Lennon, B. W., Ludwig, M. L., Wang, P. F., Veine, D. M., Becker, K., and Schirmer, R. H. (2000) *Eur. J. Biochem. 267*, 6110−6117.
3. Müller, S., Gilberger, T.-W., Färber, P. M., Becker, K., Schirmer, R. H., and Walter, R. D. (1996) *Mol. Biochem. Parasitol. 80*, 215−219.
4. Becker, K., Färber, P. M., von der Lieth, C.-W., and Müller, S. (1997) in *Flavins and Flavoproteins 1996* (Stevenson, K. J., Massey, V., and Williams, C. H., Jr., Eds.) pp 13−22, University of Calgary Press, Calgary, Alberta, Canada.
5. Gilberger, T.-W., Walter, R. D., and Müller, S. (1997) *J. Biol. Chem. 272*, 29584−29589.
6. Becker, K., Gromer, S., Schirmer, R. H., and Müller, S. (2000) *Eur. J. Biochem. 267*, 6118−6125.
7. Krnajski, Z., Gilberger, T. W., Walter, R. D., Cowman, A. F., and Müller, S. (2002) *J. Biol. Chem. 277*, 25970−25975.
8. Gromer, S., Urig, S., and Becker, K. (2003) *Med. Res. Rev.* (in press).
9. Tamura, T., and Stadtman, T. C. (1996) *Proc. Natl. Acad. Sci. U.S.A. 93*, 1006−1011.
10. Arscott, L. D., Gromer, S., Becker, K., Schirmer, R. H., and Williams, C. H., Jr. (1997) *Proc. Natl. Acad. Sci. U.S.A. 94*, 3621−3626.
11. Gilberger, T.-W., Bergmann, B., Walter, R. D., and Müller, S. (1998) *FEBS Lett. 425*, 407−410.
12. Krnajski, Z., Gilberger, T.-W., Walter, R. D., and Müller, S. (2000) *J. Biol. Chem. 275*, 40874−40878.
13. Thorpe, C., and Williams, C. H., Jr. (1976) *J. Biol. Chem. 251*, 3553−3557.
14. Pai, E. F., and Schulz, G. E. (1983) *J. Biol. Chem. 258*, 1752−1757.
15. Williams, C. H., Jr. (1992) *Chemistry and Biochemistry of Flavoenzymes* (Müller, F., Ed.) Vol. III, pp 121−211, CRC Press, Boca Raton, FL.
16. Schirmer, R. H., Krauth-Siegel, R. L., and Schulz, G. E. (1989) in *Glutathione* (Dolphin, D., Poulson, R., and Avramovic, O., Eds.) pp 553−596, John Wiley & Sons, New York.
17. Arend, M., Westermann, B., and Risch, N. (1998) *Angew. Chem., Int. Ed. 37*, 1045−1070.
18. Dimmock, J. R., Vashishtha, S. C., Quail, J. W., Pugazhenthi, U., Zimpel, Z., Sudom, A. M., Allen, T. M., Kao, G. Y., Balzarini, J., and De Clercq, E. (1998) *J. Med. Chem. 41*, 4012−4020.
19. Kanzok, S., Schirmer, R. H., Türbachova, I., Iozef, R., and Becker, K. (2000) *J. Biol. Chem. 275*, 40180−40186.
20. Wang, P.-F., Arscott, D. L., Gilberger, T.-W., Müller, S., and Williams, C. H., Jr. (1999) *Biochemistry 38*, 3187−3196.
21. Smith, D. J., Maggio, E. T., and Kenyon, G. L. (1975) *Biochemistry 14*, 766−771.
22. Williams, C. H., Jr., Arscott, L. D., Matthews, R. G., Thorpe, C., and Wilkinson, K. D. (1979) in *Methods in Enzymology: Vitamins and Coenzymes* (McCormick, D. B., and Wright, L. D., Eds.) pp 185−198, Academic Press, New York.
23. Becker, K., Herold-Mende, C., Park, J. J., Lowe, G., and Schirmer, R. H. (2001) *J. Med. Chem. 44*, 2784−2792.
24. Segel, I. H. (1975) *Enzyme Kinetics*, Wiley, London,.
25. Gromer, S., Merkle, H., Schirmer, R. H., and Becker, K. (2002) *Methods Enzymol. 347*, 382−394.
26. Dimmock, J. R., Patil, S. A., Leek, D. M., Warrington, R. C., and Fang, W. D. (1987) *Eur. J. Med. Chem. 22*, 545−551.
27. Edwards, M. L., Ritter, H. W., Stemerick, D. M., and Stewart, K. T. (1983) *J. Med. Chem. 26*, 431−436.
28. Dimmock, J. R., Smith, L. M., and Smith, P. J. (1980) *Can. J. Chem. 58*, 984−991.

29. Sandalova, T., Zhong, L., Lindqvist, Y., Holmgren, A., and Schneider, G. (2001) *Proc. Natl. Acad. Sci. U.S.A. 98*, 9533−9538.
30. Hopkins, N., and Williams, C. H., Jr. (1995) *Biochemistry 34*, 11757−11765.
31. Angiolini, L., Ghedini, N., and Tramontini, M. (1985) *Polym. Commun. 26*, 218−221.
32. Hoffman, R. D., and Lane, M. D. (1992) *J. Biol. Chem. 267*, 14005−14011.
33. Cunningham, M. L., Zvelebil, M. J., and Fairlamb, A. H. (1994) *Eur. J. Biochem. 221*, 285−295.
34. Arscott, L. D., Thorpe, C., and Williams, C. H., Jr. (1981) *Biochemistry 20*, 1513−1520.
35. Dimmock, J. R., Phillips, O. A., Wonko, S. L., Hickie, R. A., Tuer, R. G., Ambrose, S. J., Reid, R. S., Mutus, B., and Talpas, C. J. (1989) *Eur. J. Med. Chem. 24*, 217−226.
36. Mutus, B., Wagner, J. D., Talpas, C. J., Dimmock, J. R., Phillips, O. A., and Reid, R. S. (1989) *Anal. Biochem. 177*, 237−243.
37. Bauer, H., Massey, V., Arscott, L. D., Schirmer, R. H., Ballou, D. P., and Williams, C. H., Jr. (2003) *J. Biol. Chem. 278*, 33020−33028.
38. Chen, H., Ji, Z., Wong, L. K., Siuda, J. F., and Narayanan, V. L. (1994) *Bioorg. Med. Chem. 2*, 1091−1097.
39. Dimmock, J. R., Kumar, P., Quail, J. W., Pugazhenthi, U., Yang, J., Chen, M., Reid, R. S., Allen, T. M., Kao, G. Y., Cole, S. P. C., Batist, G., Balzarini, J., and De Clercq, E. (1995) *Eur. J. Med. Chem. 30*, 209−217.
40. Dimmock, J. R., Kumar, P., Nazarali, A. J., Motaganahalli, N. L., Kowalchuk, T. P., Beazely, M. A., Quail, J. W., Oloo, E. O., Allen, T. M., Szydlowski, J., De Clercq, E., and Balzarini, J. (2000) *Eur. J. Med. Chem. 35*, 967−977.
41. Baker, A., Payne, C. M., Briehl, M. M., and Powis, G. (1997) *Cancer Res. 57*, 5162−5167.
42. Boggs, S. E., McCormick, T. S., and Lapetina, E. G. (1998) *Biochem. Biophys. Res. Commun. 247*, 229−233.
43. Nicole, A., Santiard-Baron, D., and Ceballos-Picot, I. (1998) *Biomed. Pharmacother. 52*, 349−355.
44. Si, F., Ross, G. M., and Shin, S. H. (1998) *Exp. Brain Res. 123*, 263−268.
45. Powis, G., Kirkpatrick, D. L., Angulo, M., and Baker, A. (1998) *Chem.-Biol. Interact. 111−112*, 23−34.
46. Anderson, C. P., Tsai, J. M., Meek, W. E., Liu, R. M., Tang, Y., Forman, H. J., and Reynolds, C. P. (1999) *Exp. Cell Res. 246*, 183−192.
47. Higuchi, Y., and Matsukawa, S. (1999) *Arch. Biochem. Biophys. 363*, 33−42.
48. Powis, G., and Montfort, W. R. (2001) *Annu. Rev. Biophys. Biomol. Struct. 30*, 421−455.
49. Gromer, S., Johansson, L., Bauer, H., Arscott, L. D., Rauch, S., Ballou, D. P., Williams, C. H., Jr., Schirmer, R. H., and Arner, E. S. J. (2003) *Proc. Natl. Acad. Sci. U.S.A.* (in press).

BI0353629